

*J. Synchrotron Rad.* (1999), 6, 310–312

## XAFS Debye–Waller factors in aqueous Cr+3 from molecular dynamics

Luke Campbell,<sup>a\*</sup> J. J. Rehr,<sup>a</sup> Gregory K. Schenter,<sup>b</sup> Maureen I. McCarthy<sup>b</sup> and Dave Dixon<sup>b</sup>

<sup>a</sup>Department of Physics, University of Washington, Seattle, WA, 98195 U.S.A., and <sup>b</sup>Environmental Molecular Science Laboratory (MS K1-96)

Pacific Northwest National Laboratory, Richland, WA 99352.  
E-mail: lwcamp@u.washington.edu

Controversy exists on whether the second hydration shell of the aqueous chromium +3 cation is observable by XAFS. The problem is aggravated by strong first shell multiple scattering contributions competing with the second hydration shell signal. By finding *ab initio* values for nearly all free parameters in the theory, we greatly reduce the number of parameters to be fit, thus allowing an unambiguous resolution of this controversy. Quantum chemistry calculations yielded a parameterized force field model which was used in classical molecular dynamics simulations to calculate all the multiple scattering Debye–Waller factors. The self-consistent FEFF8 code fixes  $E_0$  to within 1 eV. The predicted spectrum is in good agreement with experiment. Fitted distances for the first and second hydration shell are  $2.0008 \pm 0.0068$  Å and  $3.914 \pm 0.096$  Å, respectively. The second shell is shown to be responsible for about 1/3 of the XAFS Fourier transformed signal at the position of the second shell.

**Keywords:** EXAFS; molecular dynamics; solvation; metal hydrates.

### 1. Introduction

Modern EXAFS analysis of atomic structure is based on the multiple scattering (MS) EXAFS expansion and fits a model of the signal from individual MS paths to the experiment. However, if two separate structural features generate scattering paths of similar lengths, competition between these paths can make fitting difficult. This has led to controversy over the relative importance of such paths, and to questions over whether some structural features can be seen by EXAFS at all (Filippini *et al.* 1994; Muñoz-Páez, *et al.* 1995; Sakane *et al.* 1998). As an example of such a system, the chromium +3 cation in water forms a tightly bound (inner) shell of six water molecules whose oxygen atoms form an octahedral configuration. A second (outer) shell consists of a loosely bound group of 12 to 14 water molecules at a distance close to twice that of the inner shell. Second shell single scattering paths are thus close to the same length as a number of MS paths in the first shell.

In order to overcome this complication, we have attempted to calculate most of the degrees of freedom of the MS paths of the hydrated chromium ion using a molecular dynamics (MD) simulation to account for thermal effects. MD simulations have been used in the past to investigate hydrated systems (Wallen *et al.* 1998; Kuzmin *et al.* 1997; D'Angelo *et al.* 1996; D'Angelo *et al.* 1994), but in most cases the analysis has been limited to single scattering paths. In this study, we use the MD simulation to generate a cumulant expansion in the manner of McCarthy *et al.* (1997), allowing

all MS paths to be taken into account. If the relative amplitude of all paths is known, one obtains a model with only three free parameters: an overall amplitude factor (here  $S_0^2$ ), and the distances to the oxygen atoms of the first and second hydration shells ( $R_1$  and  $R_2$ , respectively).

### 2. Approach

#### 2.1. EXAFS Equation

The EXAFS signal is given as a sum over MS paths  $i$

$$\chi(k) = \sum_i \chi_i(k) = \sum_i \text{Im} \left\{ \frac{S_0^2}{k \bar{R}_i^2} f_i^{\text{eff}}(k, \bar{R}_i) \times e^{i\phi_i + i2k\bar{R}_i - 2\sigma_i^2 k^2 - i\frac{4}{3}k^3 \sigma_i^{(3)}} \right\}$$

where  $f_i^{\text{eff}}(k, \bar{R}_i)$  is the effective scattering amplitude,  $S_0^2$  is the many body amplitude reduction factor,  $\bar{R}_i$  is the thermal averaged total distance of the scattering path,  $\sigma_i^2$  is the Debye–Waller factor, and  $\sigma_i^{(3)}$  is the third cumulant. The free parameters that must be determined are thus  $\sigma_i^2$  and  $\sigma_i^{(3)}$  for every scattering path  $i$ . In addition, one must worry about a shift in the edge energy  $E_0$  present in the theory.

#### 2.2. Electronic Structure Calculations

The first step in finding  $\sigma^2$  and  $\sigma^{(3)}$  is to parameterize the force fields that describe the molecular configurations. Density functional theory (DFT) calculations were performed on hexaaqua chromium ( $\text{Cr}(\text{H}_2\text{O})_6^{3+}$ ) in the high spin configuration by using the program DGauss (Andzelm *et al.* 1989). The geometries were optimized at the local DFT level with the DZVP2 basis set (Godbout *et al.* 1992), analytic second derivative calculations were used to show that the geometry was a true minimum and to obtain the vibrational frequencies in the harmonic approximation. The optimized bond Cr–OH<sub>2</sub> bond length is 1.965 Å. The second shell waters were added so that a symmetric configuration resulted with the oxygens of the outside water molecules facing the cluster and forming a hydrogen bond with the hydrogens of the water molecules in the first shell. Starting with this configuration, a local minimum was found using the same methods employed in the six water case.

The results of these electronic structure calculations were then used to generate a force field model to describe the intermolecular interactions, including point charges, the polarizabilities of the molecules, and a potential of the form  $-0.49454e^{-0.19508r} + 162.62e^{-2.3793r}$  for the chromium–oxygen interactions in the first hydration shell. Here, all values are in atomic units ( $e = \hbar = m_e = 1$ ), distances in Bohr, energies in Hartrees. Charge transfer is allowed in the fitting, giving a net charge of +1.5 for the chromium and –0.25 on the water molecules in the first hydration shell. The water–water interaction used the potential of Dang (1992).

#### 2.3. Molecular Dynamics Simulation

The interaction potentials and ground state configuration from the electronic structure calculations were used as input in our MD codes. These codes treat molecules as rigid bodies which interact via classical mechanics in their mutual force fields. In the chromium hydrate system, the molecules were the chromium ion and each of the eighteen water molecules. Each degree of freedom is initially given a thermal distribution corresponding to a system at 300 K. The system is then integrated over 10,000 time steps

of  $10^{-15}$  seconds each. Every ten time steps, the positions of the molecules are written to a file to obtain an ensemble of configurations of the system. Because the system is isolated, this would normally generate a microcanonical ensemble. In order to simulate a canonical ensemble, the system is rethermalized after every 100 time steps at a temperature of 300 K.

Once the ensemble is generated, the various cumulants can be calculated. Given any path between the atoms in the cluster, with  $R_i$  the total distance along path  $i$  and  $N$  the total number of configurations in the ensemble ( $N = 10^3$ ), the cumulants are

$$\begin{aligned}\bar{R}_i &= \frac{1}{N} \sum_{j=1}^N R_{i,j} \\ \sigma_i^2 &= \frac{1}{N} \sum_{j=1}^N (R_{i,j} - \bar{R}_i)^2 \\ \sigma_i^{(3)} &= \frac{1}{N} \sum_{j=1}^N R_{i,j}^3 - 3(\sigma_i^2 + \bar{R}_i^2)\bar{R}_i + 2\bar{R}_i^3.\end{aligned}$$

Higher order cumulants can be defined, and correspond to higher order corrections to the total distribution of length of the scattering path. We decided to stop at the third cumulant because a comparison of the spectrum obtained using only the first three cumulants is in excellent agreement with the spectrum generated by averaging over the spectra obtained from each configuration in the ensemble. Further details will be presented elsewhere (Campbell *et al.* to be published).

#### 2.4. EXAFS Path Expansion and $E_0$

The *ab initio* self consistent EXAFS code FEFF8 (Ankudinov *et al.* 1998) was used to find the important electron MS paths and associated scattering amplitudes. We used the ground state configuration of the hydrated chromium cluster found by the electronic structure calculation as atomic coordinates input to FEFF8. The self-consistency loop calculates the Fermi level and fixes the edge energy. The self-consistent potentials of FEFF8 appear to overestimate the signal from scattering off hydrogen atoms, which is expected to be weak. It is found that the spectrum is improved if the potentials of the oxygen atoms are calculated self-consistently in the presence of the hydrogens. For the latter, the muffin tin radii needed to be adjusted by hand to eliminate discontinuities at the muffin tin radius. The main effect of the hydrogens is a contribution in the valley between the two main peaks in  $\chi(R)$  at  $R \sim 3.3$  Å. In order to obtain the benefits of including the hydrogen while eliminating the drawbacks, the potentials were calculated in the presence of the hydrogen atoms, but MS paths involving hydrogens were not included in the path expansion. The presence of hydrogen does not effect  $E_0$  ( $E_0 = 5991.44$  eV with hydrogens, 5991.42 without hydrogens, 5991.3(3) from the experimental XANES pre-edge feature). Further details will be presented elsewhere.

#### 2.5. Data

The EXAFS spectrum of the  $\text{Cr}^{+3}$  solution in water was provided by Muñoz-Páez (private communication). The program AUTOBK (Newville *et al.* 1993) was used to find and subtract the background from the data. The resulting  $\chi(k)$  was used for fitting our model.

#### 2.6. Fitting

The fitting code FEFFIT (Stern *et al.* 1995) is used to add all the FEFF8 generated signals for the individual scattering paths. FEFFIT introduces perturbations to the zero order spectrum found by FEFF8, by considering changes in  $\bar{R}_i$ ,  $\sigma_i^2$ , and  $\sigma_i^{(3)}$  for each path  $i$ , in addition to including an amplitude reduction factor  $S_0^2$  and shift in the energy of the edge  $E_0$ . Any of these parameters can be input explicitly. Those which are unknown can be fitted to a data sample, for example. With  $\sigma^2$  and  $\sigma^{(3)}$  found by the MD codes for each path, and  $E_0$  fixed by the self-consistency routine, only  $\bar{R}$  for each path and  $S_0^2$  remain to be fitted. Since the length of the scattering path depends on the geometry of the cluster, specifying the radius of the first and second hydration shells should determine  $\bar{R}$  for every MS path. Here, the orientation between the two shells is kept fixed, and deviations in the orientation are accounted for through the effects of the cumulants  $\sigma^2$  and  $\sigma^{(3)}$ . Thus, there are only three variables to be fitted.

#### 3. Results

The fitted FT spectrum shows good agreement with the experimental data (Fig 1), showing the prominent first shell peak and a distinct peak at the second shell distance. The fitted structural parameters and those obtained by the MD simulation are shown in Table 1. Errors in the fitted parameters were estimated by FEFFIT as the change in the fitted value necessary to increase  $\chi^2$  by 1. For the MD values, the RMS error in  $\bar{R}$  is given by  $\epsilon(\bar{R}) = \sqrt{\sigma^2/(N-1)}$ . The corresponding error in  $\sigma^2$  is given by  $\epsilon(\sigma^2) = \sqrt{(\mu_4 - \mu_2^2)/N}$  for large  $N$  ( $N = 10^3$ ), where the central moment  $\mu_\nu$  is defined as  $\mu_\nu = \sum_i (R_i - \bar{R})^\nu / N$  (see, for example, Cramer, *Mathematical Methods of Statistics*, p. 348). For  $\sigma^{(3)}$ , the error could be estimated by generating values for each of several degenerate paths, and finding the RMS error of this spread of values.

Note that the distance to the second shell is slightly smaller in the fitted model than that from the MD. We believe this compression is caused by the pressure of the surrounding bulk water. That the  $\sigma^2$  found by the MD simulation is still applicable to the physical system being measured can be shown by comparing the radial distribution function of the 18 water chromium cluster and a MD simulation of the chromium ion in bulk water. Further details will be presented elsewhere.

The first shell single scattering path is by far the dominant contribution to the total signal (Fig 2). The values of  $R_1$  and  $S_0^2$  are largely determined by fitting the first shell single scattering path to the first peak. Note that this single scattering path also has significant spillover into the second peak. The first shell focusing paths, where the electron scatters from one oxygen in the first shell and is focused by the chromium ion to the opposite oxygen atom, give their main contribution in and about the second peak. There are two such paths, one in which the electron travels directly from one oxygen atom to the other, and a second in which the electron undergoes a forward scattering event off of the chromium between the two oxygen scatterings. Although individually large in amplitude, these two distinct paths largely cancel each other. This cancellation allows other, lower amplitude paths to contribute to the signal. The two other multiple scattering paths from the first shell are a triangular scattering path involving adjacent corners in the oxygen octahedron, and a backscattering path where a single oxygen is visited twice. Second shell single scattering yields a high amplitude signal, about 2/3 the total amplitude of the peak in the spectrum at the second shell distance. This signal, however, is partially can-

celed by multiple scattering paths from the first shell to the second shell of nearly the same length as the second shell SS path.

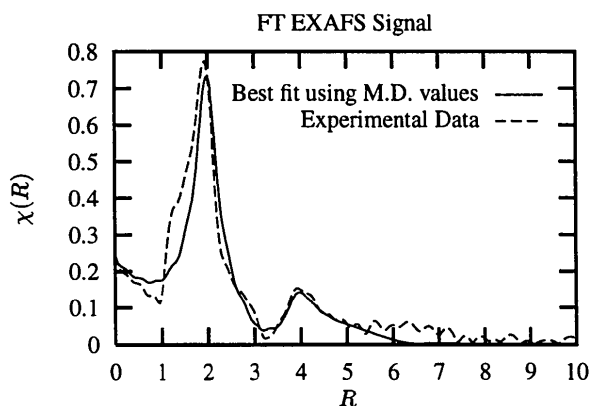


**Figure 1**  
Fourier transformed  $\chi$  from our fitted model and from the experimental data.

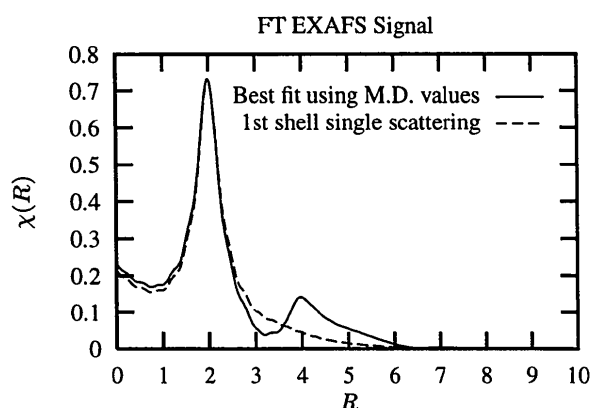


**Figure 2**  
Total  $\chi(R)$  compared to that from first shell single scattering only.

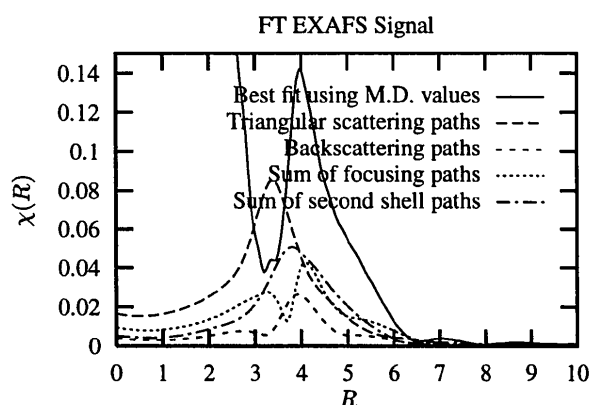


**Figure 3**  
Contribution of multiple scattering and second shell paths to the total signal.

**Table 1**  
Important Structural Features (300 K)

Feature	MD Value	Fitted Value
$\bar{R}_1$ (Å)	1.9956(17)	2.0008(68)
$\bar{R}_2$ (Å)	4.2522(66)	3.914(96)
$\sigma_1^2$ SS (Å <sup>2</sup> )	0.00296(12)	
$\sigma_2^2$ SS (Å <sup>2</sup> )	0.0436(18)	
$\sigma_1^{(3)}$ SS (Å <sup>3</sup> )	0.000026(18)	
$\sigma_2^{(3)}$ SS (Å <sup>3</sup> )	0.00052(92)	
$S_0^2$		0.821(46)

## 4. Conclusion

When diverse contributions compete to form the EXAFS spectrum, there will often be too many parameters for the spectrum to be amenable to reliable fitting. In such a case, some knowledge of the thermal damping can be used to determine their relative importance. The technique of molecular dynamic modeling allows such damping to be calculated, in addition to higher order anharmonic corrections, thus reducing the problem to one of finding a few global parameters. This method gives good results when applied to the hydrated chromium +3 system. Although our methods are different, our conclusions are comparable to those of Sakane *et al.* (1998).

The authors would like to thank A. Muñoz-Páez, E. Sánchez Marcos, and S. Díaz-Moreno for discussions which stimulated this work and for supplying the experimental data used. This work was supported by a grant from the Division of Chemical Sciences, Office of Basic Energy Sciences, U.S. Department of Energy (GKS & MIM), by DOE grant number DE-FG03-97ER45623/A000 (JJR) and by Associated Western Universities (LWC).

## References

- (a) Andzelm, J., Wimmer, E., & Salahub, D. R. in *The Challenge of d and f Electrons: Theory and Computation*, Salahub, D. R., Zemer, M. C., eds., ACS Symposium Series No 394, American Chemical Society: Washington D. C., 1989, p228. (b) Andzelm, J. in *Density Functional Theory in Chemistry*, Labanowski, J., Andzelm, J., Eds., Springer-Verlag: New York, 1991, p 155. (c) Andzelm, J. W., Wimmer, E. (1992). *J. Chem. Phys.* **96**, 1280. DGauss is a density functional program which is part of Unichem and is available from Oxford Molecular.
- Ankudinov, A. L., Ravel, B., Rehr, J. J. & Conradson, S. (1998). *Phys. Rev. B* **58** in press
- Campbell, L., Rehr, J. J., Schenter, G. K., McCarthy, M. I., & Dixon, D. to be published
- Cramer, H. *Mathematical Methods of Statistics*; Princeton university press: Princeton, 1946
- Dang, L. X. (1992). *J. Chem. Phys.* **97**, 2659.
- D'Angelo, P., Di Nola, A., Filipponi, A., Pavel, N. V., & Roccatano, D. (1994). *J. Chem. Phys.* **100**, 985-994.
- D'Angelo, P., Pavel, N. V., Roccatano, D., & Nolting, H. F. (1996). *Phys. Rev. B* **54**, 12129-38.
- Filipponi, A., D'Angelo, P., Pavel, N. V., & Di Cicco, A. (1994). *Chem. Phys. Lett.* **225**, 150-155.
- Godbout, N., Salahub, D. R., Andzelm, J., & Wimmer, E., (1992). *Can. J. Chem.* **70**, 560.
- Kuzmin, A., Obst, S., & Purans, J. (1997). *J. Phys., C.M.* **9**, 10065-78.
- McCarthy, M. I., Schenter, G. K., Chacon-Taylor, M. R., Rehr, J. J., & Brown, G. E. Jr. (1997). *Phys. Rev. B* **56**, 9925-36.
- Muñoz-Páez, A., Pappalardo, R. R., & Sánchez Marcos, E. (1995). *J. Am. Chem. Soc.* **117**, 11710-20.
- Newville, M., Livins, P., Yacoby, Y., Stern, E. A., & Rehr, J. J. (1993). *Phys. Rev. B* **47**, 14126-14131.
- Sakane, H., Muñoz-Páez, A., Díaz-Moreno, S., Martínez, J. M., Pappalardo, R. R., & Sánchez Marcos, E. (1998). *J. Am. Chem. Soc.* **120**, 10397-401.
- Stern, E. A., Newville, M., Ravel, B., Yacoby, Y., & Haskel, D. (1995). *Physica B* **208 & 209**, 117-120.
- Wallen, S. L., Palmer, B. J., & Fulton, J. L. (1998). *J. Chem. Phys.* **108**, 4039-46.

(Received 10 August 1998; accepted 21 December 1998)